

Article

Batch and Packed Bed Column Study for the Removal of Cr (VI) and Ni (II) Using Agro-Industrial Wastes

Candelaria Tejada-Tovar ¹, Angel Villabona-Ortíz ¹ and Rodrigo Ortega-Toro ^{2,*}

¹ Chemical Engineering Department, Process Design and Biomass Utilization Research Group (IDAB), University of Cartagena, Avenida del Consulado St. 30, Cartagena de Indias 130015, Colombia; tejadat@unicartagena.edu.co (C.T.-T.); avillabonao@unicartagena.edu.co (A.V.-O.)

² Department of Food Engineering, Food Packaging and Shelf Life Research Group (FP&SL) and Complex Fluids Engineering and Food Rheology Research Group (IFCRA), Universidad de Cartagena, Avenida del Consulado St. 30, Cartagena de Indias 130015, Colombia

* Correspondence: rortegap1@unicartagena.edu.co

Abstract: The objective of this study was to prepare bio adsorbents from agro-industrial wastes from yam starch (YSR) and plantain (PSR) production for its use in the removal of Cr (VI) and Ni (II) in aqueous solution in batch and continuous packed-bed column systems. Bromatological analysis showed that the biomaterials are rich in cellulose, lignin, hemicellulose, and SEM micrographs that evidence a mesoporous structure characteristic of materials of lignocellulosic origin. FTIR evidenced functional groups such as hydroxyl, carbonyl, and methyl, possibly involved in the uptake of metal ions. EDS and FTIR analysis after adsorption confirmed that the retention of the metals on the surface of the adsorbent materials was successful. Cr (VI) and Ni (II) removal efficiencies above 80% were achieved using YSR and PSR in batch systems at the different conditions evaluated. The optimum conditions for removing Ni (II) on PSR were a bed height of 11.4 cm and a temperature of 33 °C, while for YSR, they were: 43 °C and 9 cm for temperature and bed height respectively. The variable with the most significant influence on the removal of Cr (VI) in a batch system on the two bio adsorbents was temperature. In contrast, the adsorbent dose and temperature are relevant factors for PSR Ni (II) removal. Therefore, the residues from the preparation of yam and plantain starch have high potential for removing heavy metals from wastewater and are presented as an alternative for their final disposal.



Citation: Tejada-Tovar, C.; Villabona-Ortíz, A.; Ortega-Toro, R. Batch and Packed Bed Column Study for the Removal of Cr (VI) and Ni (II) Using Agro-Industrial Wastes. *Appl. Sci.* **2021**, *11*, 9355. <https://doi.org/10.3390/app11199355>

Academic Editors: Franz Jirsa and José A. López-López

Received: 13 July 2021

Accepted: 2 October 2021

Published: 8 October 2021

Publisher's Note: MDPI stays neutral with regard to jurisdictional claims in published maps and institutional affiliations.



Copyright: © 2021 by the authors. Licensee MDPI, Basel, Switzerland. This article is an open access article distributed under the terms and conditions of the Creative Commons Attribution (CC BY) license (<https://creativecommons.org/licenses/by/4.0/>).

Keywords: adsorption; biomaterials; packed bed column; adsorption kinetics

1. Introduction

Through industrialization and excessive use of chemicals worldwide, environmental pollution has resulted in heavy metals releasing into the environment and other toxic contaminants [1,2]. Heavy metals in the environment are a severe problem to address in today's world due to their high toxicity, mobility in the environment, and non-biodegradability [3]. Among them, Cr (VI) and Ni (II) are discharged in effluents from mining, electroplating, refining, and other industrial wastewaters, which can cause potential damage to the ecosystem and human and animal health, even at low concentrations [4,5]. In addition, high concentrations may cause cell membrane damage, alter enzyme activities, disrupt cell function, cause birth damage, cancer, skin lesions, and kidney and hepatic damage [6]. Cr (VI) is considered a priority dangerous pollutant since it usually occurs in the form of chromate (CrO_4^{2-}) or dichromate ($\text{Cr}_2\text{O}_7^{2-}$) ions and easily crosses biological barriers, being carcinogenic, in addition to being about 500 times more toxic and mobile than chromium (III) [7]. Ni (II), in high concentrations, is toxic and in humans, it can cause dermatitis, pulmonary fibrosis, decreased bodyweight, cardiovascular diseases, liver and kidney damage, gastrointestinal upset, and cancer [8].

For this reason, efforts have been made to remove heavy metals present in effluents through the implementation of different technologies such as solvent extraction, membrane filtration, ion exchange, reverse osmosis, chemical precipitation, oxidation, photocatalysis, among others [9]. However, these methods have limitations, such as the generation of toxic chemical sludge, incomplete metal removal, low efficiency, high energy, and reagent requirements [10].

Thus, bio adsorption is presented as a good and effective alternative technique recommended for removing heavy metal ions from water due to its low cost and ease of operation, minimal generation of toxic sludge, short operation time, the possibility of recovery, and final disposal of metals [11]. This process often uses low-cost adsorbents mainly of biological origin [12]. Various adsorbents have been tested for the removal of heavy metals from aqueous solutions with promising results based on living biomass (fungi, algae, and bacteria) and agricultural biomass (husks, sawdust, agricultural and agro-industrial wastes) [13–17]. Different lignocellulosic biomasses have been used in heavy metal removal, such as millet [18], lime [19,20], rice husks [18,21], black walnut bark [22], eucalyptus [23], palm residues [24], plantain [25], and kenaf [26], among others [27–31], presenting high removal yields. The use of bio adsorbents of residual lignocellulosic origin has advantages, such as low cost, high availability, and excellent performance at high and low concentrations [32].

Additionally, different techniques have been studied to reuse bio adsorbent materials to extend their useful life and recover the contaminants from a concentrated solution after each desorption cycle, thus using solvents as NaOH, HCl, and acetic acid, and organic solvent mixtures [33]. Regarding the final disposal of the adsorbents, once they are aged after the desorption cycles, practices have been studied to get rid of this waste, such as recycling in the cement matrix, re-filling of the road, stabilization soil, stabilization/solidification processes, and soil correction and as a liming agent, among others [34].

The large volumes of waste generated by agro-industrial exploitation require the generation of alternatives for their use. One process that produces the most waste is starch production since its yield is close to 20% [35]. Further, The Colombian national policy aimed at agricultural exploitation on the north coast and areas affected by the armed conflict to export and satisfy national consumption supposes the use of large hectares of cultivation; however, there are large volumes of post-harvest crops that do not pass the quality standards for human consumption. Thus, research was motivated around industrialization, such as the conversion to flours, for animal feed, starch, biopolymers for food packaging. Therefore, this study proposed an alternative of use for the large volumes of peel that will be generated in the biorefineries of raw materials such as yams and plantains as a product of agro-industrial rejection, seeking to take advantage of and optimize the resources and residues from said raw material [36]. Ninety percent of the yam and plantain production takes place in the departments of Bolívar, Córdoba, and Sucre, on the north Colombian coast, with about 27,938 production units of the product [36]. Therefore, the objective of the present report was to prepare bio adsorbents from yam (YSR) and plantain (PSR) starch preparation residues and evaluate their use as adsorbents of Cr (VI) and Ni (II) present in an aqueous solution in a batch and continuous system. Bio adsorbents were prepared by alkaline extraction and characterized by FTIR, SEM-EDS, and BET methods to establish the functional groups in their structure, their surface structure, and surface area. The packed-bed behavior in the continuous system was analyzed through a breakthrough curve by determining the effect of bed height and temperature over bed performance.

2. Materials and Methods

2.1. Materials

Potassium dichromate ($K_2Cr_2O_7$) and nickel sulfate ($NiSO_4$), reagent grade, were purchased from Sigma Aldrich (St. Louis, EE.UU.). The pH of the solutions was adjusted with sodium hydroxide solutions (97% purity) and 0.1 M hydrochloric acid, purchased

from Merck (Kenilworth, EE.UU.). The determination of Cr (VI) remaining concentration was carried out in a Biobase (Wolfenbüttel, Germany) UV-VIS Spectrophotometer model BK-UV1900, and Ni (II) was determined using and Perkin Elmer (Waltham, EE.UU.) Atomic Absorption spectrophotometer model 969 Solar Series with flame.

2.2. Methods

2.2.1. Biomaterials Preparation

The residual yam and plantain pulp was obtained as a reject product from the starch production process, using post-harvest agro-industrial material collected in rural areas of the department of Bolívar (Colombia). The raw material was peeled, washed with distilled water, immersed in a 0.25% *w/w* NaOH solution at 5 °C for 18 h, and filtered [17]. The particle size classification was performed in a Shaker-type sieved, Edibon Orto Alresa brand, through 2 mm and 1 mm sieves series.

2.2.2. Biomaterials Characterization

The presence of functional groups in the structure of the biomasses before and after the adsorption process was studied by Fourier transform infrared spectroscopy (FTIR) analysis using a Shimadzu (Shimadzu Corporation, Kyoto, Kyoto Prefecture, Japan) spectrophotometer model IRAinfinity-1 with 32 scans in the 400–4000 cm^{-1} spectrum; 100 mg of KBr was selected as a reference. The surface properties and elemental composition of the bio adsorbents were measured with a scanning electron microscope coupled to an energy dispersive spectroscope (SEM-EDS) provided by JEOL (Akishima, Tokyo, Japan) model JSM-6490LV. Bromatological analysis was performed to estimate carbon, hydrogen, nitrogen, ash, pectin, cellulose, hemicellulose, and lignin composition, using the following methods: AOAC 949.14, AOAC 984.13 (Kjeldahl), thermogravimetry, thermogravimetric acid digestion, thermogravimetric digestion, and photocalorimetry. Surface area, pore-volume, and pore diameter were measured by the analyzer software (ASAP 2020TM, Micrometrics, Norcross, GA, EE.UU., 2020), Micromeritics ASAP 2020, which determines the adsorption isotherm of N₂ at 195.8 °C through the BET (Brunauer, S., Emmett, P., Teller, E.) equation.

2.2.3. Experiment Design

A continuous linear factor in a central star composite response surface was selected to perform adsorption tests according to the point provided by Statgraphics Centurion Software 16.1.15 (developed by Statgraphics Technologies, Inc. (The Plains, EE.UU.)). This design allows studying the effect of the variables that influence the response by combining them simultaneously, carrying out a limited number of experiments without the need for replications, by mapping the region of a response surface [37]. Batch adsorption tests were performed on a MAXQ 4450 orbital shaker, and pH was measured on a Start A221 pH meter (Thermo Fisher Scientific brand (Waltham, EE.UU.)). The adsorption process is affected by several parameters, such as temperature, adsorbent charge, adsorbent particle size, solution pH, temperature, contact time, and agitation, among others. Previous contributions developed by the authors have suggested that the best adsorption results for Ni(II) and Cr(VI) are obtained at pH 2 and pH 6, respectively [38,39]. Thus, batch system adsorption tests were performed at 200 rpm, 30 °C, using 1 mm particle size bio adsorbents, following the composite factor design of experiments with star center point, Statgraphics Centurion Software 16.1.15 (developed by Statgraphics Technologies, Inc. (The Plains, EE.UU.)), shown Table 1.

Table 1. Experiment design: experimental ranges and various levels of the variables for the batch system tests.

Independent Variables	Unit	Range and Level				
		− α	−1	0	+1	+ α
Temperature	°C	30	40	55	70	80
Adsorbent amount	g	0.1	0.355	0.678	1	1.2
Initial concentration	mg/L	31.8	100	200	300	368.2

Experiments of continuous adsorption were carried out in an acrylic column filled with the bio adsorbent material, through which the metal solution flowed by gravity with a flow rate of 0.750 mL/s. The variables studied were bed height and temperature, following the design of experiments in Table 2. The final concentration of the ions in solution was determined by UV-VIS spectrophotometry for Cr (VI) using the 1.5-diphenylcarbazide colorimetric method at 540 nm with limit of detection of 0.096 mg/L and calibration curve correlation number of 0.999. Atomic absorption spectrophotometry was performed for Ni (II) at 232 nm, using a Thermo Fisher® Solaar S4 atomic absorption spectrometer (Waltham, MA, EE.UU.) using a nickel hollow cathode lamp, by direct determination with the flame technique; the measurement had a detection limit of 0.05 mg/L [40].

Table 2. Experiment design: experimental ranges and various levels of the variables for continuous system tests.

Independent Variables	Unit	Range and Level				
		− α	−1	0	+1	+ α
Temperature	°C	33.8	40	55	70	76.2
Bed height	Cm	1.6	3.0	6.5	10.0	11.5

2.2.4. Adsorption Study in Batch and Continuous System

The adsorption capacity (q_e) in the batch system was calculated by Equation (1), where C_o is the initial solute concentration, C_f is the final concentration after adsorption, m is the mass of adsorbent, and V is the volume of the solution.

$$q_e = \frac{(C_o - C_f) \times V}{m} \quad (1)$$

The removal efficiency (R) in batch and continuous systems was determined by Equation (2), where C_o and C_f are the initial and final solute concentrations, respectively, in mg/L. For packed-bed experiments, the sample was taken, collecting the water at the output of the column since the appearance of the first drop.

$$R = \frac{C_o - C_f}{C_o} \times 100 \quad (2)$$

The kinetic study was conducted under the best experimental conditions found, taking eight samples at different time intervals (5, 10, 15, 20, 30 min, and 1, 2, 4, 8, and 22 h) during 24 h. For this, 100 mL of solution was placed in contact with the adsorbent. The data were then fitted to the kinetic models (Pseudo-First Order and Pseudo-Second Order) using OriginPro 8.5® to calculate the fitting parameters and R^2 . Adsorption equilibrium was performed for 24 h by varying the initial concentration of contaminant (50, 100, 200, 300 mg/L). Langmuir and Freundlich's models were used to adjust the data.

The quantity of metal ions retained in the fixed-bed column were determined from the experimental breakdown curves, using Equation (3), where q_{total} is the concentration of ions in the adsorbent (mg/g), C_o is the initial concentration of the solution, and C_t is the output concentration of the ions studied in the aqueous solution (mg/L), t_s is the time it

takes for the adsorbent to convert the initial concentration to the final concentration (min), Q is the flow rate (mL/min), and m is the adsorbent mass (g) [41].

$$q_{total} = \frac{Q}{1000m} \int_0^{ts} C_t - C_o dt \quad (3)$$

3. Results and Discussion

3.1. Characterization of the Adsorbent Biomaterials

The removal of heavy metals from an aqueous solution in lignocellulosic materials is related to the presence of several functional groups on its surface (hydroxyl, carbonyl, phosphate, amino, thiol). Although their presence does not guarantee an efficient removal of metals, because this process is affected by several factors such as the number of active sites, their accessibility, chemical state, and affinity for the metal, it does depend significantly on the type of compounds and elements present, being cellulose important in lignocellulosic compounds due to its chemical stability and mechanical strength. However, it has limited free hydroxyl groups since most of them are already forming hydrogen bonds [42]. The chemical analysis shown in Table 3 corroborates the high presence of carbons, oxygens, and hydrogens in the biomasses due to the high cellulose content present in the biomasses, and to a lesser degree, lignin, and hemicellulose. It is observed that the highest lignin content occurs in the plantain residues (PSR), so it would be expected that the removal would be higher in this material [43].

Table 3. Bromatological analysis of residual plantain and yam biomasses.

Parameters (%)	PSR	YSR	Methods
Lignin	26.22	19.53	TAPPI T 222 om-83
Cellulose	41.80	39.24	TAPPI T 203 os-74
Hemicellulose	15.81	27.41	Difference between holocellulose and cellulose

Figures 1 and 2 show the IR spectra of plantain and yam starch residues, before and after the adsorption process of Cr(VI) and Ni(II), where the records between wavelengths between 3000 and 3500 cm^{-1} of O-H functional groups are initially highlighted, as well as between 3200 and 3500 cm^{-1} may appear amines and small signals of an overtone of the carbonyl by stretching vibrations of the O-H bond [44]. The peak at 2927.94 cm^{-1} is attributed to possible vibrations of C-H methyl, methylene, and methoxy groups [45], and further on between 2000 and 2500 cm^{-1} signals of alkynes and carboxylic acids can be observed as a broad signal by hydrogen bridges with overtone pattern of the carboxylic acids by O-H stretching [46]. Following this, FTIR records peaks near 1650 cm^{-1} , indicating the presence of cellulose, hemicellulose, and lignin functional groups due to C=O and C-O stretching by the vibrations of carboxyl groups of hemicellulose and lignin [32]; it can also indicate the presence of aromatic rings due to hydrogen vibrations that represent the stretching of C=C. On the other hand, between 1000 and 1200 cm^{-1} , the presence of primary, secondary and tertiary alcohols is evidenced; the product of the stretching vibrations of the C-OH bond and the bending between the plane (1225–950 cm^{-1}) are only complementary signals since the C-C, C-N, and C-O stretches fall in the same region, and several signals appear as a function of the number of hydrogens, which would affect the interactions that administered the adsorption when the adsorbate interacted with the carbonyl groups or surface alkenes of the bio sorbent [47].

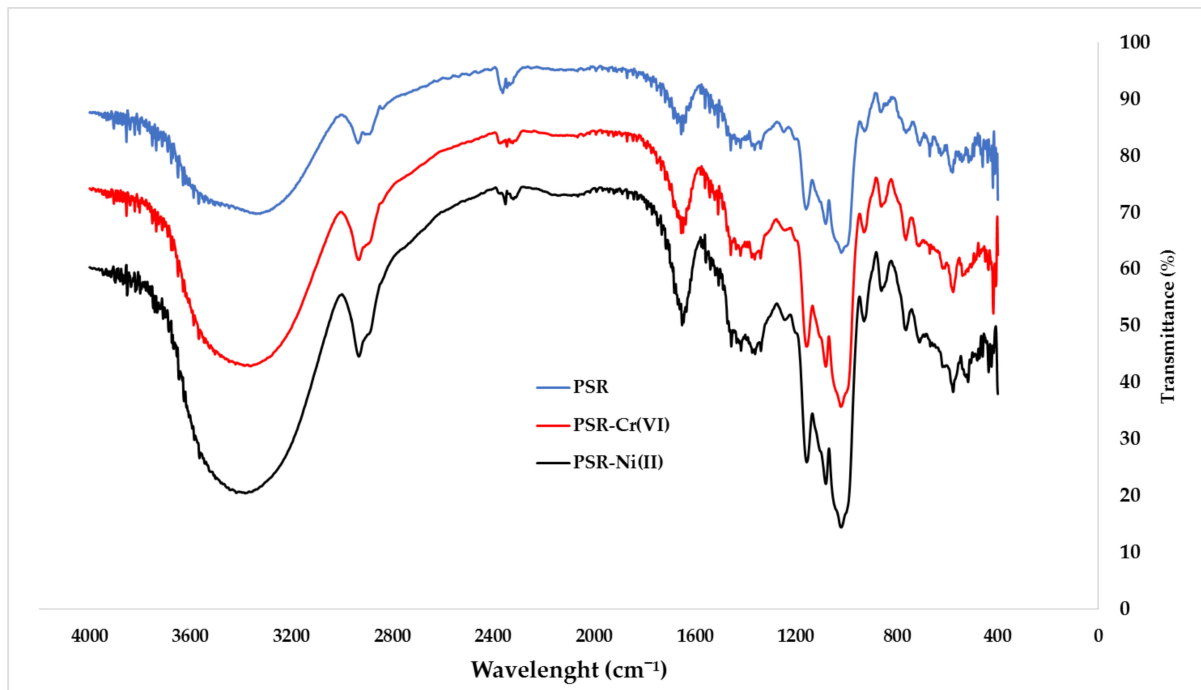


Figure 1. IR spectrum of PSR before and after Cr (VI) and Ni (II) removal.

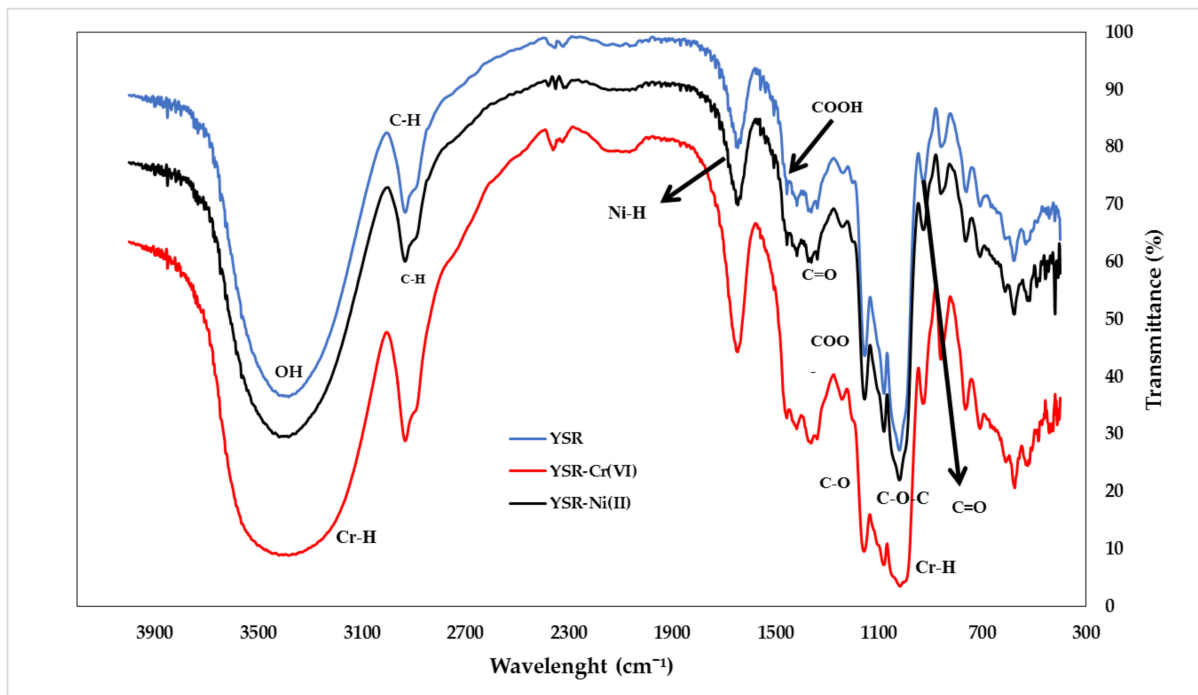


Figure 2. IR spectrum of YSR before and after removal of Cr (VI) and Ni (II).

The presence of Cr (VI) and Ni (II) metal ions within the surface structure of the biomass is evidenced in Figures 1 and 2, the increase in the width of the spectral bands and the slight decrease in intensity for each of the adsorption processes, the infrared spectroscopy after the adsorption process of Ni (II) being the one that shows a slightly more noticeable decrease in intensity. For both metals, such decrease provided by the variation of the adsorption frequency can be attributed to the binding of Cr (VI) and Ni (II) ions to the different functional groups present in the biomass, as corroborated by the change in the intensity and width of the adsorption peak at 2341 cm^{-1} , due to the interaction of hydrogen

bridges with overtone patterns indicating the presence of carboxylic acids (-COOH) [48], by O-H stretching, as shown in the change of intensity of the adsorption peak at 2927.94 cm^{-1} attributed to the vibrations of C-H methyl, methylene, and methoxy groups present in the biomass that facilitate the adsorption process and justify the high retention percentages of Cr (VI) ions at high temperatures and Ni (II) ions at ambient conditions [49].

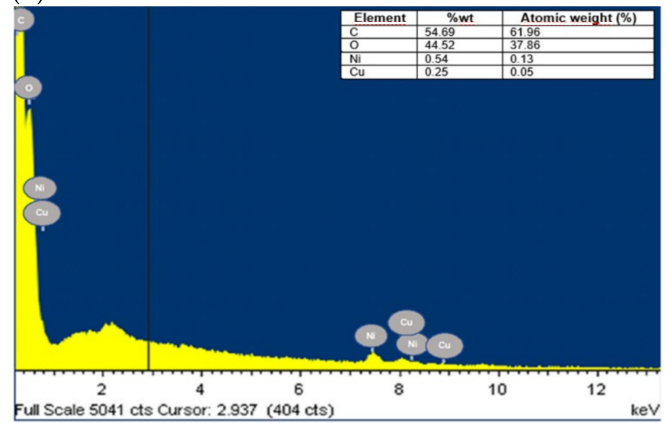
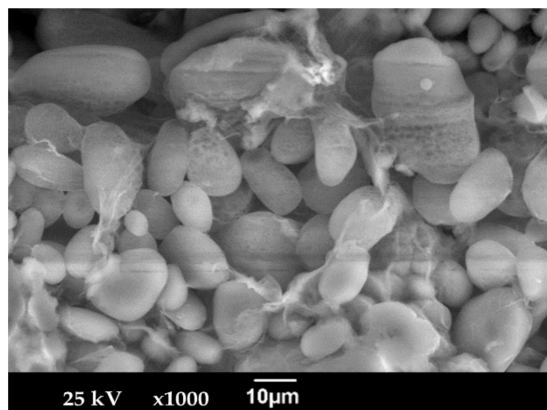
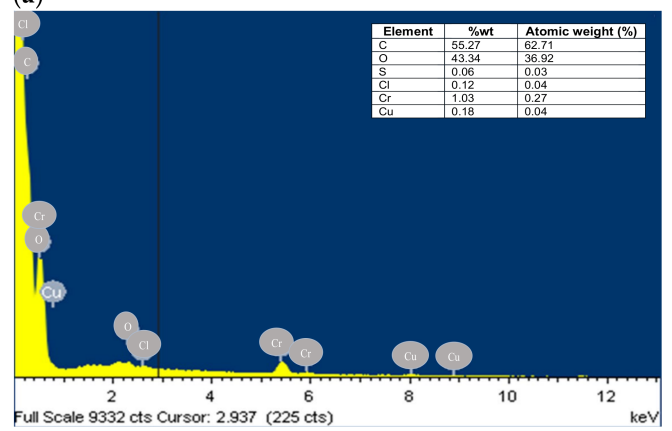
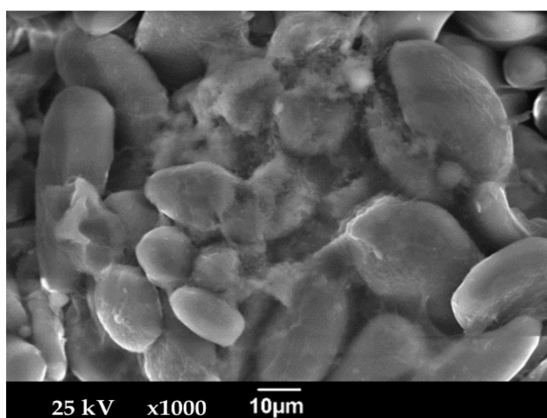
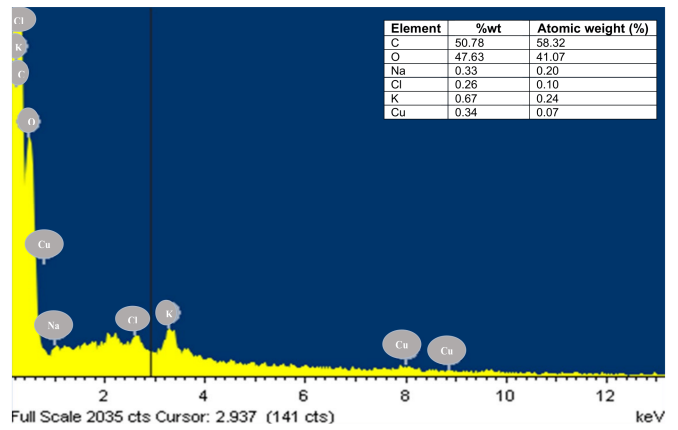
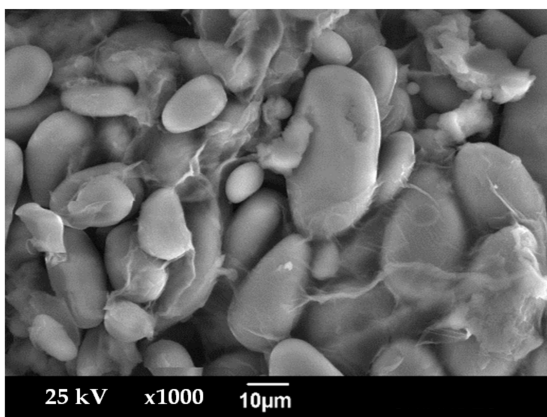
Similar to the bio adsorbents under study, other biomaterials, after the adsorption process, were characterized by FTIR and showed the presence of similar functional groups, for example, Sakura residues showed the presence of groups such as -CH, C=O, which favor Cr (VI) adsorption [50]; sugar cane bagasse showed some functional groups responsible for Ni (II) adsorption, such as, OH group attributed by a broad absorption band shown at 3350 cm^{-1} [10]. Activated coffee and coffee husk also showed the presence of the OH group due to the bands located at 1440, 1364, 698, and 626 cm^{-1} , which denotes the interaction with Ni (II) ions [51].

Adsorbent pore structure and surface chemistry contribute significantly to efficient heavy metal removal processes. Table 4 summarizes the results of the Brunauer-Emmett-Teller (BET) analysis. Plantain starch residues (PSR) reported the highest surface area; however, residues of lignocellulosic origin generally have low surface areas due to cellulose, hemicellulose, and lignin content [52]. For both biomasses, the pore volume was low; this may be due to cellulose, hemicellulose, and lignin structures within the lignocellulosic framework of the material, which may lead to the development of few numerical pores or blocked pores [53]. On the other hand, yam starch residues (YSR) presented a pore size of 83.7 nm, which makes it a macroporous biomaterial, while PSR exhibited a value between 2–50 nm, which indicates that its structure is mesoporous; this makes the bio adsorbents under study suitable for adsorption in the liquid phase since it facilitates the diffusion of the adsorbate in the adsorbent structure [54].

Table 4. Surface area and porosity analysis of biomasses.

Sample	Surface Area (m^2/g)	Pore Volume (cm^3/g)	Pore Size (nm)
PSR	38,590	0.0004	4.86
YSR	24,610	0.0055	83.71

The morphological and compositional characteristics of plantain starch residues (PSR) and yam starch residues (YSR) were analyzed. Figures 3 and 4 refer to the biomaterials before and after Cr (VI) and Ni (II) adsorption characterized by SEM analysis coupled with EDS. The micrographs showed that the surface structure of the biomaterials is uniform and cylindrical, which are attributed to the presence of lignin, hemicellulose, and cellulose [55], without micropores, as reported in Table 2 [56]. The above could be due to the alkaline extraction carried out during the preparation of the bio sorbents, increasing their adsorption capacity [57]. The EDS spectrum showed a high oxygen, carbon, and nitrogen content, which is typical of materials rich in cellulose, hemicellulose, and lignin (Table 1). Before adsorption, no signal was recorded for chromium and nickel ions. It must be said that the detection limit for bulk materials is 0.1 wt%. Therefore, EDS cannot detect trace elements (concentrations below 0.01 wt%). Thus, it can be said that the levels of Cr (VI) and Ni (II) in the bio adsorbent samples before the removal process were below the equipment limit of detection.



(c)

Figure 3. SEM micrographs and EDS of the PSR (a) natural and after adsorption of (b) Cr (VI) and (c) Ni (II).

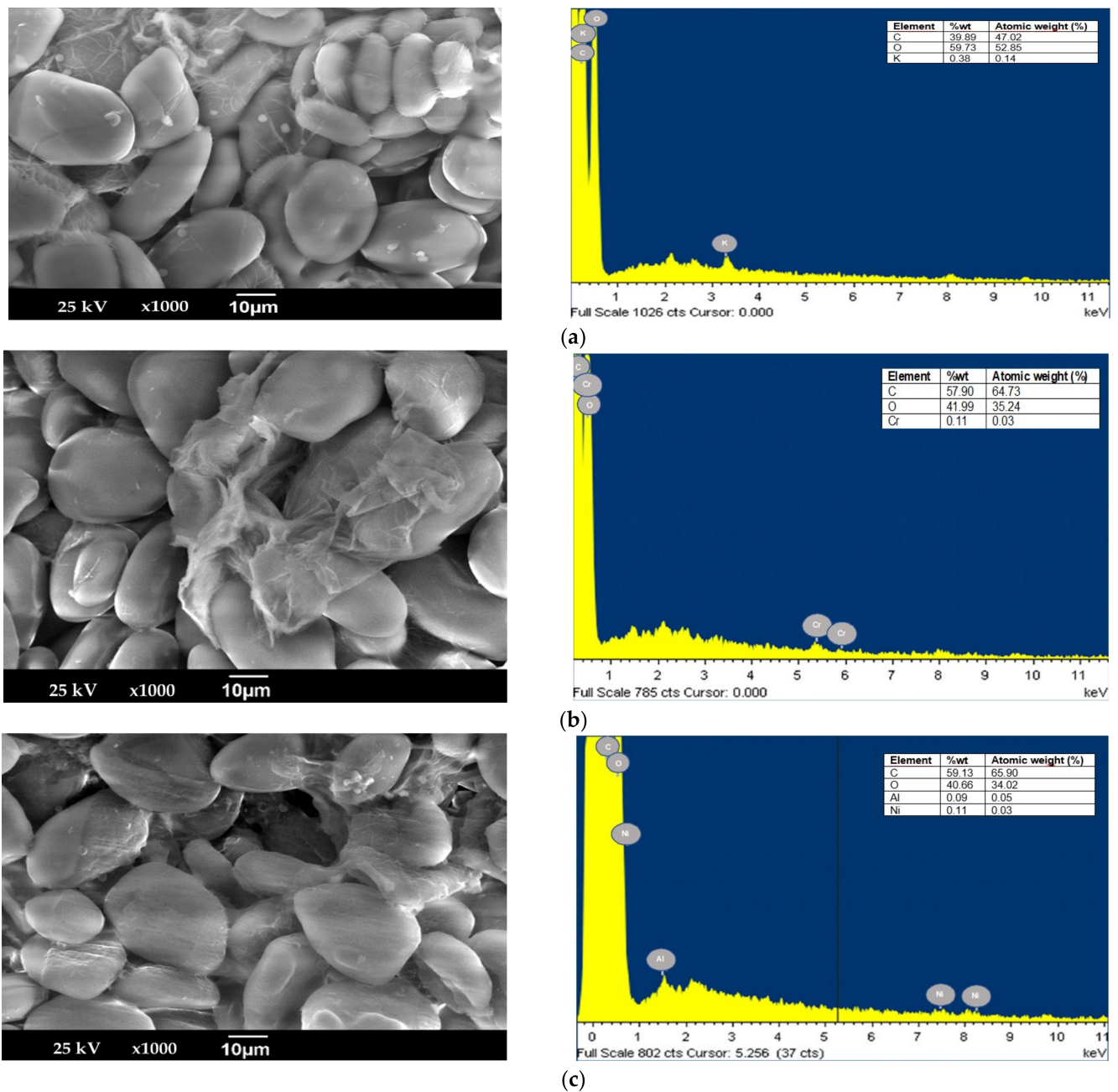


Figure 4. SEM micrographs and EDS of the YSR (a) natural and after adsorption of (b) Cr (VI) and (c) Ni (II).

SEM images of the biomaterials after adsorption of Cr (VI) and Ni (II) clearly show their smoother and more diffused structure due to the surface coverage with the metals. Previous studies report similar results when removing metals with biomaterials from *Citrus limetta* [19], *Citrus limettoides* [20], coconut sawdust, and cane bagasse [58]. After adsorption, appearance of Cr (VI) was observed in the high-intensity peaks 0.6, 5.6, and 6 keV; additionally observed were the increase of C, the decrease of O, K, and the disappearance of Na at 1 eV and K at 3.4 keV, which could be due to the formation of bonds between the ion and the active centers of the bio adsorbent [59]. Additionally, the formation of white precipitates on the material and the smoothing of the cylindrical surface are observed, which determines that ion exchange between the metals under study and the mechanism of ions in biomaterials is given by ion exchange between the metals under investigation active centers of the material [13]. Regarding the adsorption of Ni (II), we observed its appearance in the 0.8, 7.5, and 8.2 eV peaks for both biomaterials, as well as the disap-

pearance of chlorine, sodium, and potassium, which would be the active centers to which the ion adhered, with the conversation of the presence of the cover, which indicates that the adsorption of Ni (II) is highly competitive for the active centers resulting in an ion exchange process [13].

3.2. Adsorption Efficiency in Batch System

From Table 5, it is observed, from the values of p -value < 0.05 , that temperature was the variable with the most significant influence on the removal of Cr (VI) when using the biomaterials under study, as well as the amount of adsorbent when using YSR and the initial concentration of contaminant when using YSR; this can be explained since these variables are determinants on the rate of diffusion from within the solution to the active sites available on the surface and pores of the adsorbent [60]. From Table 6, it is observed that the adsorbent dose and temperature are the relevant factors in the design used for the removal of Ni (II) on PSR. At the same time, such variables are not significant when using YSR. The above shows that the processes where there is an incidence of the variables in the metal removal may be due to the interaction of adsorbate-adsorbent bonding or the formation of new effective sites for adsorption [61].

Table 5. Analysis of variance for Cr (VI) adsorption in a batch system.

Biomass	PSR			YSR		
	Source	Sum of Squares	F-Ratio	p -Value	Sum of Squares	F-Ratio
A: Temperature	158.3	0.5	0.04	997.5	8.3	0.03
B: Adsorbent dose	1302.2	3.9	0.03	132,95	1.1	0.3
C: Initial concentration	126.2	0.4	0.6	743.5	6.2	0.05
AA	58.8	0.2	0.7	51.1	0.4	0.5
AB	113.2	0.3	0.6	299.6	2.5	0.2
AC	5.0	0.02	0.9	520.5	4.4	0.08
BB	456.7	1.4	0.3	1.2	0.01	0.9
BC	43.6	0.1	0.7	231.9	1.9	0.2
CC	41.5	0.1	0.7	12.6	0.1	0.8
Total error	1976.9			718.2		
Total (corr.)	4190.4			3719.9		

Table 6. Analysis of variance for Ni (II) adsorption in a batch system.

Biomass	PSR			YSR		
	Source	Sum of Squares	F-Ratio	p -Value	Sum of Squares	F-Ratio
A: Temperature	1.9	0.09	0.8	1.6	0.06	0.8
B: Adsorbent dose	948.5	43.4	0.0012	59.3	2.3	0.3
C: Initial concentration	1490.7	68.2	0.0004	7.3	0.3	0.6
AA	38.3	1.8	0.2	7.0	0.3	0.7
AB	0.2	0.01	0.9	6.8	0.3	0.7
AC	1.52837			5.9	0.2	0.7
BB	124.6	5.7	0.06	28.6	1.1	0.4
BC	109.1	4.9	0.08	0.015	0.0	1.0
CC	207.7	9,5	0.03	0.02	0.0	1.0
Total error	109.4			50.6		
Total (corr.)	2901.7			207.7		

Regression model equations in coded form for each adsorption system in the batch system are as follows: Equation (4) is for YSR-Cr (VI), Equation (5) is for YSR-Ni (II), Equation (6) is for PSR-Cr (VI), and Equation (7) is for PSR-Ni (II). Where T is the temperature

(°C), A the adsorbent amount (g), C is the initial concentration, and q_t is the adsorption capacity (mg/g).

$$q_t = -6.01859 - 0.79674 * T + 98.0305 * A - 0.155557 * C + 0.0104372 * T^2 - 1.26502 * T * A + 0.00537723 * T * C - 3.49734 * A^2 - 0.166952 * A * C + 0.000116763 * C^2 \quad (4)$$

$$q_t = -4.6956 - 23.224 * A + 0.6779 * T + 0.0484 * C - 6.6834 * A^2 + 0.7036 * M * T + 0.0146 * A * C - 0.0037 * T^2 - 0.0029 * T * C + 0.0002 * C^2 \quad (5)$$

$$q_t = 325.826 - 68.131 * A - 6.8846 * T - 1.0124 * C + 153.937 * A^2 - 3.7751 * A * T + 0.2585 * A * C + 0.6677 * T^2 + 0.0129 * T * C + 0.00034 * C^2 \quad (6)$$

$$q_t = 63.7897 - 0.0362617 * C - 1.1754 * T - 60.2943 * A + 0.0006 * C^2 - 0.0003 * C * T - 0.1145 * C * A + 0.0112 * T^2 - 0.03176 * T * A + 43.6142 * A^2 \quad (7)$$

For continuous systems, regression model equations were generated too, and these are as follows: Equation (8) is for YSR-Cr (VI), Equation (9) is for YSR-Ni (II), Equation (10) is for PSR-Cr (VI), and Equation (11) is for PSR-Ni (II). Where H is the bed height (cm), T is the temperature (°C), and R is the efficiency of removal (%).

$$R = 3.42 * 10^{-6} - 6.94 * T - 3.62 * 10^8 * T - 3.61 * 10^9 * H + 2.76 * 10^6 * T^2 + 4.73 * 10^7 * T * H + 5.069 * 10^7 * H^2 \quad (8)$$

$$R = 23.11 + 1.22 * T + 10.90 * H - 0.006 * T^2 - 0.081 * T * H - 0.41 * H^2 \quad (9)$$

$$R = -75.343 + 1.442 * H^2 + 3.384 * T - 0.006 * H^2 - 0.006 * H * T - 0.020 * T^2 \quad (10)$$

$$R = 93.001 + 0.043 * T + 0.092 * H - 0.0002 * T^2 - 0.0006 * T * H - 0.0003 * H^2 \quad (11)$$

The equations make it possible to establish the influence of each evaluated effect and their interactions as standardized values.

The removal efficiencies were calculated by Equation (1) after the adsorption process shown in Figure 5. PSR biomass reported high removal efficiencies (>80%) for the removal of Cr (VI) and Ni (II) ions, which can be attributed to the high surface area and small pore size enhancing adsorption properties of such materials [62], consistent with the EDS after the adsorption process reported in Figures 4 and 5, as well as the irregular morphologies evidenced in the SEM micrographs, which is a desirable characteristic of adsorbents due to the availability of active sites for adsorbing heavy metal ions [63].

The kinetic study was carried out to analyze the effect of time on the adsorption capacity at the best experimental conditions found for each process (Table 7). According to these best experimental conditions, a gap of 10 °C between optimum conditions for removing Ni (II) onto both bio adsorbents. This fact could be explained because the structure of PSR is dominated by the presence of mesopores (Table 4 and Figure 3), while the size of the pores of YSR is macro (Table 4 and Figure 4); these results suggest an excellent adsorbent capacity by PSR, as it could offer a larger contact area between the metal ions and the biomaterial [64]. On the other hand, the increase in temperature is possibly explained by the endothermic nature of the Ni (II) adsorption process, and it may be due to the increase in the ionization of the lignocellulosic components, which act as adsorption sites, thus promoting the increase in the rate of diffusion of Ni (II) through the outer boundary layer into the pores [65,66].

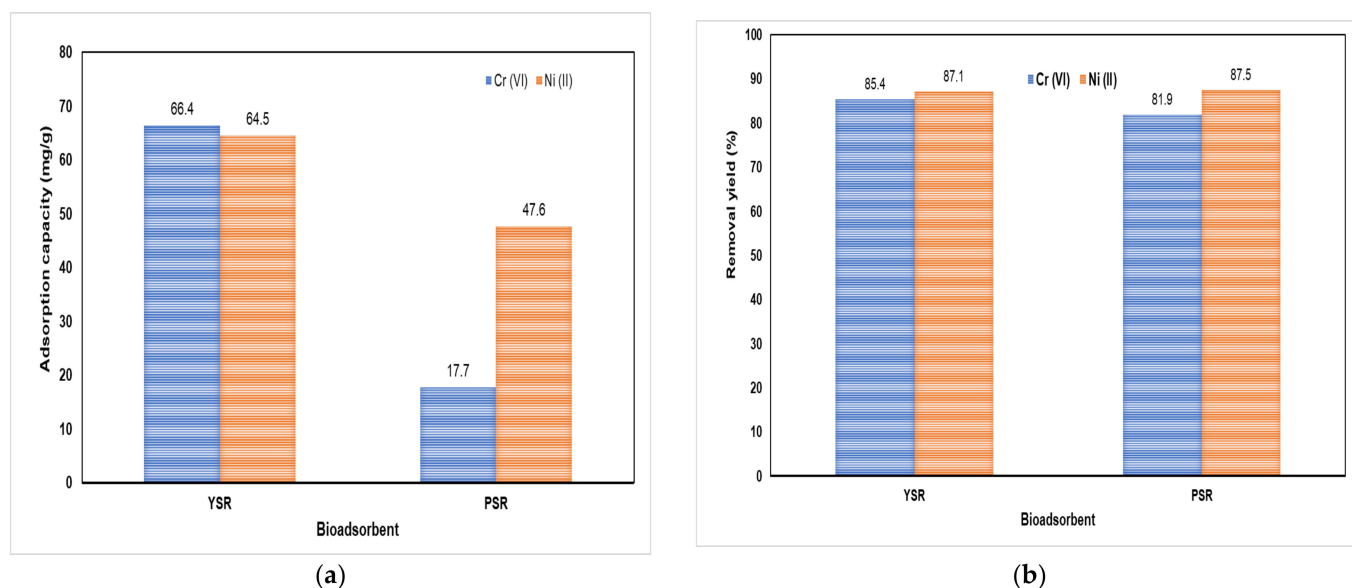


Figure 5. Results of Cr (VI) and Ni (II) adsorption on biomass-derived adsorbents. $n = 1$. (a) Adsorption capacity; (b) Removal efficiency.

Table 7. Best adsorption conditions for Cr (IV) and Ni (II) on YSR and PSR.

Adsorbent	Metal	Temperature (°C)	Adsorbent Dose (g)	Initial Concentration (mg/L)
YSR	Cr (VI)	76.16	0.14	368.18
	Ni (II)	70	1.19	31.82
PSR	Cr (VI)	40	1	100
	Ni (II)	55	0.6775	368.18

The fit parameters of the pseudo-first-order and pseudo-second-order models were estimated by nonlinear fitting and are summarized in Table 8. It was found that the pseudo-second-order model best describes the adsorption kinetics of the two metals under study on YSR and PSR according to the correlation coefficient obtained; this indicates that the removal of metals occurs by chemisorption or chemical adsorption due to the formation of chemical bonds between adsorbent and adsorbate [67]. The value of the k_2 constant evidences the selectivity of the materials for Cr (VI) relatively to Ni (II), which could be explained by the difference in the electronic configuration, ionic radius, and first ionization potential of the two metals. [68]. According to the pseudo-second-order parameter k_2 , it was observed that Cr (VI) ion was adsorbed at a faster rate than Ni (II). This fact may be explained by considering the ionic radius of both metals: Ni (II) (0.72 Å) y Cr (VI) (0.52 Å). Since Cr (VI) ions have a smaller ionic radius, it could be reasonable that their faster diffusion could be possible through the adsorbent pores [69]. Additionally, it showed the selectivity of PSR by Ni (II) ions, which has been speculated to the availability of limiting binding surface sites [70]. Concerning q_e calculated parameters by pseudo-first and pseudo-second-order model, it is observed quite a difference between the obtained parameters by each model, as well as R^2 , having pseudo-second-order more accuracy with experimental data; this may be due to the chemical nature of the interactions between the metal ions and adsorbent active sorption centers [33].

Table 8. Kinetic model fitting parameters.

Model	Parameter	PSR		YSR	
		Cr (VI)	Ni (II)	Cr (VI)	Ni (II)
Pseudo-first-order	q_{e1} (mg/g)	9.65	18.54	75.8	105.3
	k_1 (min^{-1})	4.92	0.12	1.7×10^{12}	8.2×10^{12}
	R^2	0.99	0.96	0.78	0.97
Pseudo-second-order	q_{e2} (mg/g)	9.73	19.24	94.6	112.9
	k_2 (g/mg min)	2.99	0.012	3.49	2.24
	R^2	0.99	0.98	0.98	0.99

The fitting parameters of the isotherm models are summarized in Table 9. The Freundlich model achieved the R^2 closest to 1, indicating the heterogeneity of the bio adsorbent surfaces, which is consistent with the results obtained during the biomass characterizations (Figures 1 and 2). Likewise, the adsorption process occurs in multilayer due to the non-uniform heat distribution in the pores of the adsorbents [71]. The Freundlich constant value, n , of 12.82 suggests that there are strong bonds between the Cr (VI) ions and the YSR surface and that the adsorption process is favorable [72].

Table 9. Fitting parameters of isotherm models.

Model	Parameter	PSR		YSR	
		Cr (VI)	Ni (II)	Cr (VI)	Ni (II)
Langmuir	q_{max} (mg/g)	44,021.46	27,775.59	77.5	3.86×10^8
	b (L/mg)	3.67×10^{-6}	1.6256×10^5	2.9	3.9×10^{38}
	R^2	0.94	0.99	0.92	0.08
Freundlich	k_F (mg/g)	0.013	0.14	54.2	8.7×10^{-15}
	n	0.63	0.99	12.8	0.49
	R^2	0.97	0.99	0.96	0.99

3.3. Packed Bed Column Performance

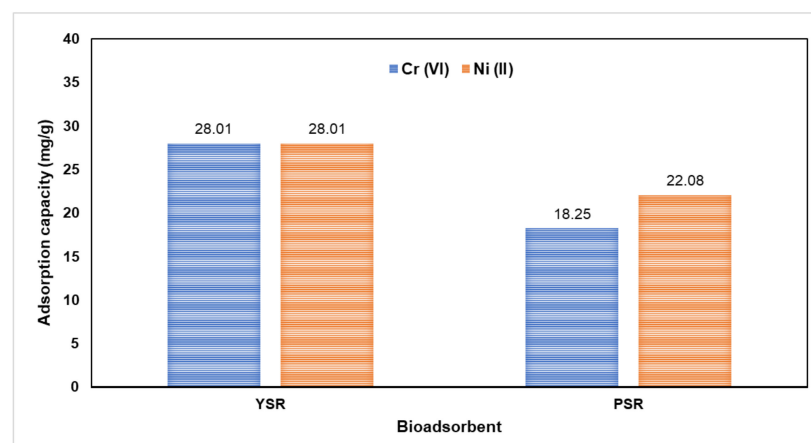
Table 10 shows the results obtained for the study of the influence of temperature and bed height on the removal efficiency of Cr (VI) and Ni (II) on PSR and YSR; for this experiment, a concentration of 100 mg/L was taken as the initial condition. The adsorption percentage was calculated using Equation (2). For the removal of Cr (VI) on PSR, a positive effect of the increase in temperature was evidenced, which can be caused by the increase in the diffusion rate of the ions in the mesopores of the adsorbent due to the formation of bonds with the groups; likewise, the increase in the bed height benefits the removal due to the greater availability of the active centers and the residence time; consequently, the metal has more time to diffuse in the solid phase [73]. Thus, the best conditions for removing Cr (VI) using PSR are a bed height of 8.14 cm and a temperature of 68 °C. When using YSR to remove Cr (VI), it is evident that the temperature and bed height conditions do not seem to influence the process since percentages >90% were obtained in almost all cases. Therefore, it can be concluded that the lower bed height (1.5 cm) and the ambient temperature (30 °C) are sufficient to favor the adsorbent-adsorbate contact area.

Table 10. Removal efficiencies of Cr (VI) and Ni (II) on PSR and YSR in a continuous system.

Bed Height (cm)	Temperature (°C)	PSR		YSR	
		Cr (VI)	Ni (II)	Cr (VI)	Ni (II)
6.5	33	65.67	98.13	79.91	94.31
10.0	40	82.45	98.28	99.91	99.03
3.0	40	63.51	94.81	99.36	81.75
11.5	55	94.78	96.73	99.91	91.60
6.5	55	92.37	97.20	98.85	97.85
1.6	55	54.87	97.13	97.58	81.49
10.0	70	94.78	97.15	99.49	95.52
3.0	70	89.19	95.00	99.36	95.25
6.5	76	95.42	97.01	99.91	93.76

For Ni (II) removal, removal efficiencies >80% were obtained at the different conditions evaluated using the two bio adsorbents; all obtained values were within the calibration curve and above the detection limit. The lowest adsorption values were obtained using YSR at 40 °C/3 cm and 55 °C/1.5 cm, respectively, with an efficiency of 81%. It is also evident that the bed height has a direct influence, thus favoring the adsorption efficiency of Ni (II) present in the solution; this is because the greater the amount of adsorbent in the column, the more binding sites are available, thus expanding the mass transfer zone [74]. When the bed height is low, axial dispersion phenomena predominate during mass transfer, which reduces the residence time and the rate of diffusion of ions from the solution to the adsorbent [73]. Thus, it was found that the optimum conditions for removing Ni (II) on PSR were a bed height of 11.4 cm and a temperature of 33 °C, while for YSR, they were: 43 °C and 9 cm for temperature and bed height respectively.

The breakthrough curve, which describes the behavior of the adsorbate concentration concerning time for the pollutant load leaving the bed, was determined at the best conditions previously specified to achieve maximum removal in the packed column configuration and operation of the adsorption tests in order to establish the useful life and breakthrough or saturation point of the bed over 8 continuous hours [75], where the saturation of the biomass in the adsorption column was observed for an initial concentration of 100 mg/L. Figure 6 shows the maximum adsorption capacities in the packed bed system of Cr (VI) and Ni (II) on YSR and PSR calculated with Equation (3). Better performance of YSR for the removal of the two metals was observed, which could be attributed to its larger pore size and volume (Table 4) for PSR. Other authors found Ni (II) adsorption capacity of 54 mg/g on a *Bacillus* sp. bio composite supported on alginate and revealed that the increase in bed height and initial concentration resulted in a higher adsorption rate and higher biosorption rate [76].

**Figure 6.** Experimental packed-bed column capacity. $n = 1$.

It is emphasized that the present study was limited to adsorption experiments of Cr (VI) and Ni (II) ions on two materials obtained as rejection product of the starch-obtaining process, using yam and plantain as raw materials, in a batch and continuous system. Desorption cycles were not carried out. However, the use of hydrochloric and nitric acids in concentrations ranging from 0.1 to 1 M was studied to evaluate the reuse of adsorbents and recovery of heavy metals from lignocellulosic matrices [32]. However, the final disposal of saturated biomasses with heavy metals remains a challenge. Thus, different immobilization techniques based on cement or brick have been studied as an attractive solution to this problem. In addition, the presence of soluble organic compounds in treated water presents another field for future research. A considerable difference was observed between the maximum experimental capacity obtained by the filter (Figure 6) and the calculated by Langmuir's model (Table 9).

4. Conclusions

It is concluded that: (a) The biomaterials are rich in cellulose, lignin, and hemicellulose and have a mesoporous structure characteristic of materials of lignocellulosic origin. (b) FTIR evidenced functional groups such as hydroxyl, carbonyl, and methyl, possibly involved in the uptake of metal ions. (c) EDS and FTIR analyses confirmed that the retention of metals on the surface of the adsorbent materials was successful. (d) Cr (VI) and Ni (II) removal efficiencies above 80% were achieved using YSR and PSR in batch systems at the different conditions evaluated. (e) The variable with the most significant influence on removing Cr (VI) in a batch system on the two bio adsorbents was temperature. In contrast, the adsorbent dose and temperature were the relevant factors for Ni (II) removal on PSR. (f) From the fitting of the kinetics data to the pseudo-second-order model, it is inferred that adsorption occurs by chemical adsorption. (g) The fitting of the adsorption equilibrium to the Freundlich model indicated that the process occurs in multilayers. (h) The batch and continuous study evidenced a better performance of YSR due to the larger pore size and volume compared with PSR. This study is presented as an alternative for the final disposal of residues from the process of obtaining starch from yam and plantain; its use as a biomaterial represents a solution to mitigate Cr (VI) and Ni (II) contamination in water. The observed results are based only on specific configurations of the experiments.

Author Contributions: Conceptualization, C.T.-T.; data curation, A.V.-O. and R.O.-T.; formal analysis, C.T.-T.; funding acquisition, C.T.-T. and A.V.-O.; methodology, C.T.-T.; project administration, A.V.-O.; software, A.V.-O.; supervision, C.T.-T.; validation, A.V.-O.; visualization, R.O.-T.; writing—original draft, C.T.-T.; writing—review and editing, R.O.-T. All authors have read and agreed to the published version of the manuscript.

Funding: This research received no external funding.

Institutional Review Board Statement: Not applicable.

Informed Consent Statement: Not applicable.

Data Availability Statement: The data presented in this study are available on request from the corresponding authors.

Acknowledgments: The authors express their gratitude to Universidad de Cartagena for providing equipment and reagents to conduct this research.

Conflicts of Interest: The authors declare no conflict of interest.

References

1. Naik, R.M.; Ratan, S.; Singh, I. Use of orange peel as an adsorbent for the removal of Cr (VI) from its aqueous solution. *Indian J. Chem. Technol.* **2018**, *25*, 300–305.
2. Bharagava, R.N.; Chowdhary, P. Textile wastewater dyes: Toxicity profile and treatment approaches. In *Emerging and Eco-Friendly Approaches for Waste Management*; Springer: Berlin/Heidelberg, Germany, 2018; pp. 1–435, ISBN 9789811086694.
3. Mishra, S.; Bharagava, R.N. Toxic and genotoxic effects of hexavalent chromium in environment and its bioremediation strategies. *J. Environ. Sci. Health Part C* **2016**, *34*, 1–32. [[CrossRef](#)]

4. Xia, S.; Song, Z.; Jeyakumar, P.; Shaheen, S.M.; Rinklebe, J.; Ok, Y.S.; Bolan, N.; Wang, H. A critical review on bioremediation technologies for Cr(VI)-contaminated soils and wastewater. *Crit. Rev. Environ. Sci. Technol.* **2019**, *49*, 1027–1078. [[CrossRef](#)]
5. Genchi, G.; Carocci, A.; Lauria, G.; Sinicropi, M.S.; Catalano, A. Nickel: Human health and environmental toxicology. *Int. J. Environ. Res. Public Health* **2020**, *17*, 679. [[CrossRef](#)]
6. Peng, S.H.; Wang, R.; Yang, L.Z.; He, L.; He, X.; Liu, X. Biosorption of copper, zinc, cadmium and chromium ions from aqueous solution by natural foxtail millet shell. *Ecotoxicol. Environ. Saf.* **2018**, *165*, 61–69. [[CrossRef](#)]
7. Corral-Escárcega, M.C.; Ruiz-Gutiérrez, M.G.; Quintero-Ramos, A.; Meléndez-Pizarro, C.O.; Lardizabal-Gutiérrez, D.; Campos-Venegas, K. Use of biomass-derived from pecan nut husks (*Carya illinoensis*) for chromium removal from aqueous solutions. column modeling and adsorption kinetics studies. *Rev. Mex. Ing. Quim.* **2017**, *16*, 939–953.
8. Chowdhury, Z.Z.; Zain, S.M.; Rashid, A.K.; Rafique, R.F.; Khalid, K. Breakthrough curve analysis for column dynamics sorption of Mn(II) ions from wastewater by using *Mangostana garcinia* peel-based granular-activated carbon. *J. Chem.* **2013**, *2013*, 959761. [[CrossRef](#)]
9. Bhanvase, B.A.; Ugwekar, R.P.; Mankar, R.B. *Novel Water Treatment and Separation Methods: Simulation of Chemical Processes*; Apple Academic Press, INC: Waretown, NJ, USA, 2017; ISBN 9781315225395.
10. Ezeonuegbu, B.A.; Machido, D.A.; Whong, C.M.Z.; Japhet, W.S.; Alexiou, A.; Elazab, S.T.; Qusty, N.; Yaro, C.A.; Batiha, G.E.S. Agricultural waste of sugarcane bagasse as efficient adsorbent for lead and nickel removal from untreated wastewater: Biosorption, equilibrium isotherms, kinetics and desorption studies. *Biotechnol. Rep.* **2021**, *30*, e00614. [[CrossRef](#)]
11. Villabona-Ortiz, A.; Tejada-Tovar, C.; González-Delgado, Á.D.; Herrera-Barros, A.; Cantillo-Arroyo, G. Immobilization of lead and nickel ions from polluted yam peels biomass using cement-based solidification/stabilization technique. *Int. J. Chem. Eng.* **2019**, *2019*, 5413960. [[CrossRef](#)]
12. Sadeghalvad, B.; Khorshidi, N.; Azadmehr, A.; Sillanpää, M. Sorption, mechanism, and behavior of sulfate on various adsorbents: A critical review. *Chemosphere* **2021**, *2021*, 263. [[CrossRef](#)] [[PubMed](#)]
13. Xia, L.; Xu, X.; Zhu, W.; Huang, Q.; Chen, W. A comparative study on the biosorption of Cd²⁺ onto *Paecilomyces lilacinus* XLA and *Mucoromycote* sp. XLC. *Int. J. Mol. Sci.* **2015**, *16*, 15670–15687. [[CrossRef](#)]
14. Yuan, W.; Cheng, J.; Huang, H.; Xiong, S.; Gao, J.; Zhang, J.; Feng, S. Optimization of cadmium biosorption by *Shewanella putrefaciens* using a Box-Behnken design. *Ecotoxicol. Environ. Saf.* **2019**, *175*, 138–147. [[CrossRef](#)] [[PubMed](#)]
15. Pennesi, C.; Amato, A.; Occhialini, S.; Critchley, A.T.; Totti, C.; Giorgini, E.; Conti, C.; Beolchini, F. Adsorption of indium by waste biomass of brown alga *Ascophyllum nodosum*. *Sci. Rep.* **2019**, *9*, 1–11. [[CrossRef](#)]
16. Magoling, B.J.A.; Macalalad, A.A. Removal of Chromium (VI) from Aqueous Solution. *J. Environ. Manag.* **2017**, *12*, 3001–3016.
17. Wang, F.; Pan, Y.; Cai, P.; Guo, T.; Xiao, H. Single and binary adsorption of heavy metal ions from aqueous solutions using sugarcane cellulose-based adsorbent. *Bioresour. Technol.* **2017**, *241*, 482–490. [[CrossRef](#)]
18. Batagarawa, S.M.; Ajibola, A.K. Comparative evaluation for the adsorption of toxic heavy metals on to millet, corn and rice husks as adsorbents. *J. Anal. Pharm. Res.* **2019**, *8*, 119–125. [[CrossRef](#)]
19. Singh, S.; Shukla, S.R. Theoretical studies on adsorption of Ni(II) from aqueous solution using Citrus limetta peels. *Environ. Prog. Sustain. Energy* **2017**, *36*, 864–872. [[CrossRef](#)]
20. Sudha, R.; Srinivasan, K.; Premkumar, P. Removal of Nickel (II) from aqueous solution using Citrus Limettioides peel and seed carbon. *Ecotoxicol. Environ. Saf.* **2015**, *117*, 115–123. [[CrossRef](#)]
21. Janyasuthiwong, S.; Phiri, S.M.; Kijjanapanich, P.; Rene, E.R.; Esposito, G.; Lens, P.N.L. Copper, lead and zinc removal from metal-contaminated wastewater by adsorption onto agricultural wastes. *Environ. Technol.* **2015**, *36*, 3071–3083. [[CrossRef](#)] [[PubMed](#)]
22. Lawal, O.S.; Ayanda, O.S.; Rabiou, O.O.; Adebowale, K.O. Application of black walnut (*Juglans nigra*) husk for the removal of lead (II) ion from aqueous solution. *Water Sci. Technol.* **2017**, *75*, 2454–2464. [[CrossRef](#)] [[PubMed](#)]
23. Haroon, H.; Ashfaq, T.; Gardazi, S.M.H.; Sherazi, T.A.; Ali, M.; Rashid, N.; Bilal, M. Equilibrium kinetic and thermodynamic studies of Cr(VI) adsorption onto a novel adsorbent of *Eucalyptus camaldulensis* waste: Batch and column reactors. *Korean J. Chem. Eng.* **2016**, *33*, 2898–2907. [[CrossRef](#)]
24. Nordin, N.; Asmadi, N.A.A.; Manikam, M.K.; Halim, A.A.; Hanafiah, M.M.; Hurairah, S.N. Removal of hexavalent chromium from aqueous solution by adsorption on palm oil fuel ash (POFA). *J. Geosci. Environ. Prot.* **2020**, *8*, 112–127. [[CrossRef](#)]
25. Villabona-Ortiz, Á.; Tejada-Tovar, C.; Ruiz-Paternina, E.; Frías-González, J.D.; Blanco-García, G.D. Optimization of the effect of temperature and bed height on Cr (VI) bioadsorption in continuous system. *Rev. Fac. Ing.* **2020**, *29*, e10477. [[CrossRef](#)]
26. Omidvar-Borna, M.; Pirsahab, M.; Vosoughi-Niri, M.; Khosravi-Mashizie, R.; Kakavandi, B.; Zare, M.R.; Asadi, A. Batch and column studies for the adsorption of chromium(VI) on low-cost *Hibiscus Cannabinus* kenaf, a green adsorbent. *J. Taiwan Inst. Chem. Eng.* **2016**, *68*, 80–89. [[CrossRef](#)]
27. Raval, N.P.; Shah, P.U.; Shah, N.K. Adsorptive removal of nickel (II) ions from aqueous environment: A review. *J. Environ. Manage.* **2016**, *179*, 1–20. [[CrossRef](#)] [[PubMed](#)]
28. Carolin, C.F.; Kumar, P.S.; Saravanan, A.; Joshiba, G.J.; Naushad, M. Efficient techniques for the removal of toxic heavy metals from aquatic environment: A review. *Biochem. Pharmacol.* **2017**, *5*, 2782–2799. [[CrossRef](#)]
29. Neris, J.B.; Luzardo, F.H.M.; da Silva, E.G.P.; Velasco, F.G. Evaluation of adsorption processes of metal ions in multi-element aqueous systems by lignocellulosic adsorbents applying different isotherms: A critical review. *Chem. Eng. J.* **2019**, *357*, 404–420. [[CrossRef](#)]

30. Bolisetty, S.; Peydayesh, M.; Mezzenga, R. Sustainable technologies for water purification from heavy metals: Review and analysis. *Chem. Soc. Rev.* **2019**, *48*, 463–487. [[CrossRef](#)]
31. Hu, X.; Xue, Y.; Liu, L.; Zeng, Y.; Long, L. Preparation and characterization of Na₂S-modified biochar for nickel removal. *Environ. Sci. Pollut. Res.* **2018**, *25*, 9887–9895. [[CrossRef](#)] [[PubMed](#)]
32. Priyantha, N.; Lim, L.B.L.; Mallikarathna, S.; Kulasoorya, T.P.K. Enhanced removal of Ni(II) by acetic acid-modified peat. *Desalin. Water Treat.* **2019**, *137*, 162–173. [[CrossRef](#)]
33. Nkuigie Fotsing, P.; Bouazizi, N.; Djoufac Woumfo, E.; Mofaddel, N.; Le Derf, F.; Vieillard, J. Investigation of chromate and nitrate removal by adsorption at the surface of an amine-modified cocoa shell adsorbent. *J. Environ. Chem. Eng.* **2021**, *9*, 104618. [[CrossRef](#)]
34. Zhang, S.; Zhao, Y.; Guo, Z.; Ding, H. Stabilization/solidification of hexavalent chromium containing tailings using low-carbon binders for cemented paste backfill. *J. Environ. Chem. Eng.* **2021**, *9*, 104738. [[CrossRef](#)]
35. Tejada-Tovar, R.E.; Tejada-Benítez, L.P.; Tejada-Tovar, C.; Villabona-Ortíz, A.; Granados-Conde, C. Aprovechamiento de ñame espinoso post-cosecha (*Dioscorea rotundata* P.) en la extracción de ácido láctico. *Rev. Prospect.* **2018**, *16*, 76–82. [[CrossRef](#)]
36. Mendoza-Crespo, H.; Ortiz-Velásquez, M. Importance and determinants of the agricultural productive association: Yam cultivation in the Colombian Caribbean. *Soc. Y Econ.* **2020**, 88–108. [[CrossRef](#)]
37. Demirel, M.; Kayan, B. Application of response surface methodology and central composite design for the optimization of textile dye degradation by wet air oxidation. *Int. J. Ind. Chem.* **2012**, *3*, 1–10. [[CrossRef](#)]
38. Herrera-Barros, A.; Bitar-Castro, N.; Villabona-Ortíz, Á.; Tejada-Tovar, C.; González-Delgado, Á.D. Nickel adsorption from aqueous solution using lemon peel biomass chemically modified with TiO₂ nanoparticles. *Sustain. Chem. Pharm.* **2020**, *17*, 100299. [[CrossRef](#)]
39. Tejada-Tovar, C.; Villabona-Ortiz, A.; Ruiz-Paternina, E. Cinética de adsorción de Cr (VI) usando biomásas residuales modificadas químicamente en sistemas por lotes y continuo. *Rev. Ion.* **2015**, *28*, 29–41.
40. Şaylan, M.; Zaman, B.T.; Gülhan Bakırdere, E.; Bakırdere, S. Determination of trace nickel in chamomile tea and coffee samples by slotted quartz tube-flame atomic absorption spectrometry after preconcentration with dispersive liquid-liquid microextraction method using a Schiff base ligand. *J. Food Compos. Anal.* **2020**, *88*, 103454. [[CrossRef](#)]
41. Kavand, M.; Fakoor, E.; Mahzoon, S.; Soleimani, M. An improved film-pore-surface diffusion model in the fixed-bed column adsorption for heavy metal ions: Single and multi-component systems. *Process. Saf. Environ. Prot.* **2018**, *113*, 330–342. [[CrossRef](#)]
42. Šoštarić, T.D.; Petrović, M.S.; Pastor, F.T.; Lončarević, D.R.; Petrović, J.T.; Milojković, J.V.; Stojanović, M.D. Study of heavy metals biosorption on native and alkali-treated apricot shells and its application in wastewater treatment. *J. Mol. Liq.* **2018**, *259*, 340–349. [[CrossRef](#)]
43. Rinaldi, R.; Yasdi, Y.; Hutagalung, W.L.C. Removal of Ni (II) and Cu (II) ions from aqueous solution using rambutan fruit peels (*Nephelium lappaceum* L.) as adsorbent. *AIP Conf. Proc.* **2018**, 2026. [[CrossRef](#)]
44. Tatah, V.S.; Ibrahim, K.L.C.; Ezeonu, C.S.; Otitoju, O. Biosorption kinetics of heavy metals from fertilizer industrial waste water using groundnut husk powder as an adsorbent. *J. Appl. Biotechnol. Bioeng.* **2017**, *2*, 221–228. [[CrossRef](#)]
45. Khalil, U.; Shakoob, M.B.; Ali, S.; Ahmad, S.R.; Rizwan, M.; Alsahli, A.A.; Alyemini, M.N. Selective removal of hexavalent chromium from wastewater by rice husk: Kinetic, isotherm and spectroscopic investigation. *Water* **2021**, *13*, 263. [[CrossRef](#)]
46. Ranasinghe, S.H.; Navaratne, A.N.; Priyantha, N. Enhancement of adsorption characteristics of Cr(III) and Ni(II) by surface modification of jackfruit peel biosorbent. *J. Environ. Chem. Eng.* **2018**, *6*, 5670–5682. [[CrossRef](#)]
47. Ghorbani, F.; Kamari, S.; Zamani, S.; Akbari, S.; Salehi, M. Optimization and modeling of aqueous Cr(VI) adsorption onto activated carbon prepared from sugar beet bagasse agricultural waste by application of response surface methodology. *Surf. Interfaces* **2020**, *18*, 100444. [[CrossRef](#)]
48. Hanafiah, S.F.M.; Salleh, N.F.M.; Ghafar, N.A.; Shukri, N.M.; Kamarudin, N.H.N.; Hapani, M.; Jusoh, R. Efficiency of coconut husk as agricultural adsorbent in removal of chromium and nickel ions from aqueous solution. *IOP Conf. Ser. Earth Environ. Sci.* **2020**, *596*, 012048. [[CrossRef](#)]
49. Zafar, S.; Imran Khan, M.; Khraisheh, M.; Hussain Lashari, M.; Shahida, S.; Farooq Azhar, M.; Prapamonthon, P.; Latif Mirza, M.; Khalid, N.; Jammu, A. Kinetic, equilibrium and thermodynamic studies for adsorption of nickel ions onto husk of *Oryza sativa*. *Desalin. Water Treat.* **2019**, *167*, 277–290. [[CrossRef](#)]
50. Qi, W.; Zhao, Y.; Zheng, X.; Ji, M.; Zhang, Z. Adsorption behavior and mechanism of Cr(VI) using Sakura waste from aqueous solution. *Appl. Surf. Sci.* **2016**, *360*, 470–476. [[CrossRef](#)]
51. Hernández Rodríguez, M.; Yperman, J.; Carleer, R.; Maggen, J.; Daddi, D.; Gryglewicz, G.; Van der Bruggen, B.; Falcón Hernández, J.; Otero Calvis, A. Adsorption of Ni(II) on spent coffee and coffee husk based activated carbon. *J. Environ. Chem. Eng.* **2018**, *6*, 1161–1170. [[CrossRef](#)]
52. Asuquo, E.; Martin, A.; Nzerem, P.; Siperstein, F.; Fan, X. Adsorption of Cd(II) and Pb(II) ions from aqueous solutions using mesoporous activated carbon adsorbent: Equilibrium, kinetics and characterisation studies. *J. Environ. Chem. Eng.* **2017**, *5*, 679–698. [[CrossRef](#)]
53. Asuquo, E.D.; Martin, A.D. Sorption of cadmium (II) ion from aqueous solution onto sweet potato (*Ipomoea batatas* L.) peel adsorbent: Characterisation, kinetic and isotherm studies. *J. Environ. Chem. Eng.* **2016**, *4*, 4207–4228. [[CrossRef](#)]
54. Berhe, S.; Ayele, D.; Tadesse, A.; Mulu, A. Adsorption efficiency of coffee husk for removal of lead (II) from industrial effluents: Equilibrium and kinetic study. *Int. J. Sci. Res. Publ.* **2015**, *5*, 753–859.

55. Wu, H.; Liu, Z.; Yang, H.; Li, A. Evaluation of chain architectures and charge properties of various starch-based flocculants for flocculation of humic acid from water. *Water Res.* **2016**, *96*, 126–135. [[CrossRef](#)]
56. Song, W.; Gao, B.; Guo, Y.; Xu, X.; Yue, Q.; Ren, Z. Effective adsorption/desorption of perchlorate from water using corn stalk based modified magnetic biopolymer ion exchange resin. *Microporous Mesoporous Mater.* **2017**, *252*, 59–68. [[CrossRef](#)]
57. Schwantes, D.; Gonçalves, A.C.; Campagnolo, M.A.; Tarley, C.R.T.; Dragunski, D.C.; de Varennes, A.; dos Santos Silva, A.K.; Conradi, E. Chemical modifications on pinus bark for adsorption of toxic metals. *J. Environ. Chem. Eng.* **2018**, *6*, 1271–1278. [[CrossRef](#)]
58. Pranata Putra, W.; Kamari, A.; Najiah Mohd Yusoff, S.; Fauziah Ishak, C.; Mohamed, A.; Hashim, N.; Md Isa, I. Biosorption of Cu(II), Pb(II) and Zn(II) ions from aqueous solutions using selected waste materials: Adsorption and characterization studies. *J. Encapsulation Adsorpt. Sci.* **2014**, *4*, 25–35. [[CrossRef](#)]
59. Cherdchoo, W.; Nithettham, S.; Charoenpanich, J. Removal of Cr(VI) from synthetic wastewater by adsorption onto coffee ground and mixed waste tea. *Chemosphere* **2019**, *221*, 758–767. [[CrossRef](#)] [[PubMed](#)]
60. Ajmani, A.; Shahnaz, T.; Subbiah, S.; Narayanasamy, S. Hexavalent chromium adsorption on virgin, biochar, and chemically modified carbons prepared from Phanera vahlii fruit biomass: Equilibrium, kinetics, and thermodynamics approach. *Environ. Sci. Pollut. Res.* **2019**, *26*, 32137–32150. [[CrossRef](#)]
61. Ruiz-Paternina, E.B.; Villabona-Ortiz, Á.; Tejada-Tovar, C.; Ortega-Toro, R. Estudio termodinámico de la remoción de níquel y cromo en solución acuosa usando adsorbentes de origen agroindustrial. *Inf. Tecnol.* **2019**, *30*, 3–10. [[CrossRef](#)]
62. Bibaj, E.; Lysigaki, K.; Nolan, J.W.; Seyedsalehi, M.; Deliyanni, E.A.; Mitropoulos, A.C.; Kyzas, G.Z. Activated carbons from banana peels for the removal of nickel ions. *Int. J. Environ. Sci. Technol.* **2019**, *16*, 667–680. [[CrossRef](#)]
63. De Melo, N.H.; de Oliveira Ferreira, M.E.; Silva Neto, E.M.; Martins, P.R.; Ostroski, I.C. Evaluation of the adsorption process using activated bone char functionalized with magnetite nanoparticles. *Environ. Nanotechnol. Monit. Manag.* **2018**, *10*, 427–434. [[CrossRef](#)]
64. Liu, Q.S.; Zheng, T.; Li, N.; Wang, P.; Abulikemu, G. Modification of bamboo-based activated carbon using microwave radiation and its effects on the adsorption of methylene blue. *Appl. Surf. Sci.* **2010**, *256*, 3309–3315. [[CrossRef](#)]
65. Mushtaq, M.; Nawaz, H.; Iqbal, M.; Noreen, S. Eriobotrya japonica seed biocomposite efficiency for copper adsorption: Isotherms, kinetics, thermodynamic and desorption studies. *J. Environ. Manag.* **2016**, *176*, 21–33. [[CrossRef](#)]
66. Renugadevi, N.; Rajalakshmi, R.; Subhashini, S.; Lalitha, P.; Malarvizhi, T. Usefulness of activated carbon prepared from agro waste in the removal of dyes from aqueous solution. *Indian J. Environ. Prot.* **2009**, *29*, 250–254.
67. Egbosiuba, T.C.; Abdulkareem, A.S.; Kovo, A.S.; Afolabi, E.A.; Tijani, J.O.; Bankole, M.T.; Bo, S.; Roos, W.D. Adsorption of Cr(VI), Ni(II), Fe(II) and Cd(II) ions by KIAgNPs decorated MWCNTs in a batch and fixed bed process. *Sci. Rep.* **2021**, *11*, 75. [[CrossRef](#)] [[PubMed](#)]
68. Mansouri, H.; Carmona, R.J.; Gomis-Berenguer, A.; Souissi-Najar, S.; Ouederni, A.; Ania, C.O. Competitive adsorption of ibuprofen and amoxicillin mixtures from aqueous solution on activated carbons. *J. Colloid Interface Sci.* **2015**, *449*, 252–260. [[CrossRef](#)]
69. Abia, A.; Asuquo, E. Lead (II) and nickel (II) adsorption kinetics from aqueous metal solutions using chemically modified and unmodified agricultural adsorbents. *Afr. J. Biotechnol.* **2009**, *5*, 1475–1482. [[CrossRef](#)]
70. Islam, M.A.; Aual, M.R.; Angove, M.J. A review on nickel(II) adsorption in single and binary component systems and future path. *J. Environ. Chem. Eng.* **2019**, *7*, 103305. [[CrossRef](#)]
71. Negm, N.A.; Abd, M.G.; Wahed, E.; Rahman, A.; Hassan, A.; Abou, M.T.H. Feasibility of metal adsorption using brown algae and fungi: Effect of biosorbents structure on adsorption isotherm and kinetics Feasibility of metal adsorption using brown algae and fungi: Effect of biosorbents structure on adsorption isotherm and kine. *J. Mol. Liq.* **2018**, *264*, 292–305. [[CrossRef](#)]
72. Rodrigues, E.; Almeida, O.; Brasil, H.; Moraes, D.; Reis, M.A.L. Applied clay science adsorption of chromium (VI) on hydrotalcite-hydroxyapatite material doped with carbon nanotubes: Equilibrium, kinetic and thermodynamic study. *Appl. Clay Sci.* **2019**, *172*, 57–64. [[CrossRef](#)]
73. Amirnia, S.; Ray, M.B.; Margaritis, A. Copper ion removal by Acer saccharum leaves in a regenerable continuous-flow column. *Chem. Eng. J.* **2016**, *287*, 755–764. [[CrossRef](#)]
74. Jafari, S.A.; Jamali, A. Continuous cadmium removal from aqueous solutions by seaweed in a packed-bed column under consecutive sorption-desorption cycles. *Korean J. Chem. Eng.* **2016**, *33*, 1296–1304. [[CrossRef](#)]
75. Banerjee, M.; Bar, N.; Basu, R.K.; Das, S.K. Removal of Cr(VI) from its aqueous solution using green adsorbent pistachio shell: A fixed bed column study and GA-ANN modeling. *Water Conserv. Sci. Eng.* **2018**, *3*, 19–31. [[CrossRef](#)]
76. Naskar, A.; Majumder, R.; Goswami, M.; Mazumder, S.; Maiti, S.; Ray, L. Implication of greener biocomposite bead for decontamination of Nickel(II): Column dynamics Study. *J. Polym. Environ.* **2020**, *28*, 1985–1997. [[CrossRef](#)]